J Eng Math (2006) 56:221–235
DOI 10.1007/s10665-006-9080-z

ORIGINAL PAPER

A generalization of prolate spheroidal functions with more uniform resolution to the triangle

Mark A. Taylor · Beth A. Wingate

Received: 9 January 2006 / Accepted: 18 July 2006 /
Published online: 28 September 2006

Abstract Prolate spheroidal functions constitute a one-parameter (α) family of orthogonal functions in the interval. For $\alpha = 0$, they are the Legendre polynomials. For larger α, the prolate spheroidal functions oscillate more uniformly than the Legendre polynomials, and provide more uniform resolution in the interval. The prolate spheroidal functions can be obtained by adding a zeroth-order term to the Sturm–Liouville equation for the Legendre polynomials. Here, the Sturm–Liouville equation for orthogonal polynomials in the triangle is modified in a similar fashion. The modification maintains the self-adjointness and symmetry properties of the original Sturm–Liouville equation, so that the new eigenfunctions are orthogonal and give spectrally accurate approximations of smooth functions with arbitrary boundary conditions in the triangle. The properties of the new eigenfunctions mimic those in the interval. For larger α, the new eigenfunctions provide more uniform resolution in the triangle.

Keywords Prolate spheroidal · Triangle · Sturm Liouville · Polynomial approximation

1 Introduction

There has been recent interest in using prolate spheroidal wave functions (PSWFs) for the numerical solution of partial differential equations [1–5]. The PSWFs are a one-parameter (α) family of orthogonal functions in the interval $[-1, 1]$ generalizing the Legendre polynomials. For the bandwidth parameter $\alpha = 0$, the wave functions are the Legendre polynomials. For values of the bandwidth parameter $\alpha > 0$, new families of PSWFs are generated that are no longer polynomials; oscillate more uniformly than the Legendre polynomials and provide more uniform resolution over $[-1, 1]$. In the references mentioned above, more uniform resolution is demonstrated by showing that the expansion of sinusoids in a truncated

M. A. Taylor (✉)
Sandia National Laboratories, Albuquerque, NM, USA
e-mail: mataylo@sandia.gov

B. A. Wingate
Los Alamos National Laboratory, Los Alamos, NM, USA
e-mail: wingate@lanl.gov

series of $\alpha > 0$ PSWFs is significantly more accurate than that obtained with a similar number of Legendre polynomials. Furthermore, the associated collocation points for finite truncations of PSWFs are found to be more uniformly spaced.

The PSWFs can be obtained from a modification of the Sturm–Liouville equation for the Legendre polynomials. They are the eigenfunctions of

$$\frac{\partial}{\partial x}\left((1-x^2)\frac{\partial u}{\partial x}\right) - \alpha^2 x^2 u = \lambda u \tag{1}$$

in the interval $[-1,1]$. For $\alpha = 0$, this is the classical Sturm–Liouville equation for the Legendre polynomials.

Here we generalize this construction by making a similar modification to the Sturm–Liouville equation whose eigenfunctions are orthogonal polynomials in two variables over the triangle. To generalize this equation, we are careful to preserve three key properties:

1. *Symmetry*. The equation should be invariant under the symmetry group of the domain. For the interval $[-1,1]$ this simply means the equation is invariant under a change in sign of x. For the triangle, we require the equation be invariant under D_3, the group of rotations and reflections of the triangle onto itself. This is so that the eigenfunctions will not, for example, provide more resolution in one corner of the triangle compared to the remaining corners.
2. *Self-adjointness*. If the operator is self-adjoint, classic Sturm–Liouville theory gives us a complete set of orthogonal eigenfunctions. We also preserve the singular nature of the Sturm–Liouville equation, meaning that the operator is self-adjoint over a space of functions with no imposed boundary conditions or periodicity. This is all that is required to preserve a key property of the $\alpha = 0$ polynomial expansions: for $f \in C^\infty$, the truncated eigenfunction expansion of f will converge to f faster than any polynomial, with no boundary requirements on f.
3. *Form of the bandwidth term* $\alpha^2 x^2 u$. In the triangle, we preserve the quadratic and invariant form of this term on the belief that this term will also generate eigenfunctions which, for $\alpha > 0$, provide more uniform resolution in the triangle as compared to polynomials.

In Sect. 2, we construct a second-order differential operator $\mathcal{L}$ in the triangle with all three of the above properties. The bandwidth parameter is introduced by analogy with the one-dimensional Sturm–Liouville equation for PSWFs. In Sect. 3, we use a spectral method to solve for the eigenvectors and eigenfunctions of this generalized equation. Results are given in Sect. 4, where we demonstrate that, as with PSWfs, the resulting eigenfunctions do indeed have more uniform resolution.

2 Construction of a Sturm–Liouville problem in the triangle

We start by constructing differential operators in the equilateral triangle, as shown in Fig. 1. We construct our operators in this triangle so that their symmetry properties are easily shown, but then map the equilateral triangle to the right triangle where the equation is more easily solved.

2.1 The triangles T_e and T_r

Let T_e represent the interior of the triangle, as given by the intersection of $y > -\frac{1}{2}$, $y < -\sqrt{3}x + 1$ and $y < \sqrt{3}x + 1$. The vertices are $(0,1)$, $(-\frac{\sqrt{3}}{2}, -\frac{1}{2})$ and $(\frac{\sqrt{3}}{2}, -\frac{1}{2})$.

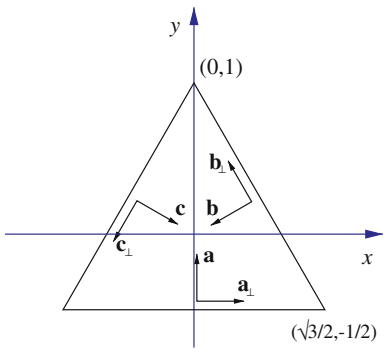

Fig. 1 Edge-based coordinate systems in the equilateral triangle T_e. The **a** coordinate system is aligned with the Cartesian coordinates x and y. The unit vectors are given by $\hat{\mathbf{a}} = (0,1)$ and $\hat{\mathbf{a}}_\perp = (1,0)$. The **b** and **c** coordinate systems are obtained by rotating the **a** coordinate system 120° counterclockwise or clockwise

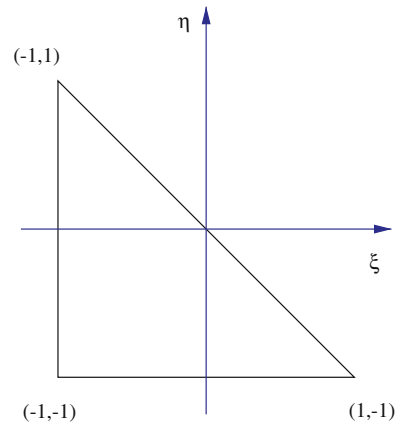

Fig. 2 The right triangle T_r

We first construct a coordinate system aligned with each edge of the triangle, as shown in Fig. 1. The unit vectors for these coordinate systems are given by

$$\hat{\mathbf{a}} = (0,1), \quad \hat{\mathbf{b}} = \left(-\frac{\sqrt{3}}{2}, -\frac{1}{2}\right), \quad \hat{\mathbf{c}} = \left(\frac{\sqrt{3}}{2}, -\frac{1}{2}\right),$$

$$\hat{\mathbf{a}}_\perp = (1,0), \quad \hat{\mathbf{b}}_\perp = \left(-\frac{1}{2}, \frac{\sqrt{3}}{2}\right), \quad \hat{\mathbf{c}}_\perp = \left(-\frac{1}{2}, -\frac{\sqrt{3}}{2}\right).$$

We represent a point $\mathbf{r} = (x,y)$ in the three coordinate systems by $\mathbf{r} = a\hat{\mathbf{a}} + a_\perp\hat{\mathbf{a}}_\perp = b\hat{\mathbf{b}} + b_\perp\hat{\mathbf{b}}_\perp = c\hat{\mathbf{c}} + c_\perp\hat{\mathbf{c}}_\perp$.

We denote the group of rotations and reflections of T_e onto itself by D_3. The rotations of the point $a\hat{\mathbf{a}} + a_\perp\hat{\mathbf{a}}_\perp$ are given by $\{a\hat{\mathbf{a}} + a_\perp\hat{\mathbf{a}}_\perp, a\hat{\mathbf{b}} + a_\perp\hat{\mathbf{b}}_\perp, a\hat{\mathbf{c}} + a_\perp\hat{\mathbf{c}}_\perp\}$ and its reflections are $\{a\hat{\mathbf{a}} - a_\perp\hat{\mathbf{a}}_\perp, a\hat{\mathbf{b}} - a_\perp\hat{\mathbf{b}}_\perp, a\hat{\mathbf{c}} - a_\perp\hat{\mathbf{c}}_\perp\}$. Thus, to show that a differential operator is invariant under D_3, we need only show that it is invariant under permutations of the three edge-based coordinate systems and under change of sign of edge-normal coordinate.

For convenience, our numerical calculations will be performed by mapping the equations given in T_e into the right triangle T_r as shown in Fig. 2. To avoid confusion with the Cartesian coordinates used in T_e, we denote the Cartesian coordinates in the right triangle by (ξ,η). The linear map between T_r and T_e is given in Appendix A.2. The Jacobian is $\frac{3\sqrt{3}}{8}$, and the integrals are related by

$$\iint_{T_e} f(x,y)\,\mathrm{d}x\,\mathrm{d}y = \frac{3\sqrt{3}}{8}\iint_{T_r} f(x(\xi,\eta), y(\xi,\eta))\mathrm{d}\xi\,\mathrm{d}\eta.$$

2.2 A second-order invariant self-adjoint operator $\mathcal{L}$

We define the differential operators

$$\frac{\partial}{\partial a_\perp} = \hat{\mathbf{a}}_\perp \cdot \nabla, \quad \frac{\partial}{\partial b_\perp} = \hat{\mathbf{b}}_\perp \cdot \nabla, \quad \frac{\partial}{\partial c_\perp} = \hat{\mathbf{c}}_\perp \cdot \nabla, \tag{2}$$

where ∇ is the usual Cartesian gradient. We now consider the following second-order differential operator,

$$\mathcal{L}_a(u) = \frac{\partial}{\partial a_\perp}\left(p(a,a_\perp)\frac{\partial u}{\partial a_\perp}\right). \tag{3}$$

We first note that, if $p(a,a_\perp)$ is chosen to vanish along the edges of the triangle perpendicular to $\hat{\mathbf{b}}$ and $\hat{\mathbf{c}}$ and positive in T_e, then $\mathcal{L}_a$ will be negative definite and self-adjoint in $H^2(T_e)$ (functions in T_e with square-integrable second derivatives). The proof is by straightforward integration by parts and is given in Appendix A.1. Note that, because $\mathcal{L}_a$ is singular at the boundary, no boundary conditions need to be imposed on the functions $f \in H^2(T_e)$.

To choose a function p, we consider the lowest-degree polynomial that vanishes on the desired edges, $p(a,a_\perp) = ((a-1)^2 - 3a_\perp^2)$. It is easy to check that $p(a,a_\perp) > 0\ \forall (a,a_\perp) \in T_e$, as shown in Appendix A.2.

We define $\mathcal{L}_b$ and $\mathcal{L}_c$ as identical operators, but expressed in the **b** and **c** coordinate systems, respectively. Since these operators are just rotations of $\mathcal{L}_a$, they are also self-adjoint in T_e. Now consider the operator

$$\mathcal{L} = \frac{1}{3}\left(\mathcal{L}_a + \mathcal{L}_b + \mathcal{L}_c\right). \tag{4}$$

This operator is self-adjoint, since it is the sum of self-adjoint operators. To see that $\mathcal{L}$ is invariant under D_3, we consider the action of D_3 on $\mathcal{L}_a$. The rotations by 0, 120 and 240 degrees are expressed by $\mathcal{L}_a, \mathcal{L}_b$ and $\mathcal{L}_c$, respectively. The reflection of $\mathcal{L}_a$ about $\hat{\mathbf{a}}$ changes the sign of $\hat{\mathbf{a}}_\perp$ which leaves $\mathcal{L}_a$ unchanged. Reflection of $\mathcal{L}_a$ about $\hat{\mathbf{b}}$is equivalent to rotation of $\hat{\mathbf{a}}$ into $\hat{\mathbf{c}}$ followed by reflection about $\hat{\mathbf{c}}$, which gives $\mathcal{L}_c$. Similarly, reflection of $\mathcal{L}_a$ about $\hat{\mathbf{c}}$ gives $\mathcal{L}_b$. Thus the action of D_3 on $\mathcal{L}$ is given by permutations of the subscripts a,b,c, all of which leave $\mathcal{L}$ unchanged.

2.3 Eigenfunctions and eigenvalues of $\mathcal{L}$

We now describe the eigenfunctions and eigenvalues of the Sturm–Liouville problem

$$\mathcal{L}(u) = \frac{1}{3}\left(\mathcal{L}_a(u) + \mathcal{L}_b(u) + \mathcal{L}_c(u)\right) = \lambda u \tag{5}$$

with $p(a,a_\perp) = (a-1)^2 - 3a_\perp^2$. This equation can be solved analytically by first mapping the equilateral to the right triangle T_r. The algebra needed to express $\mathcal{L}$ in Cartesian coordinates in T_r and T_e is given in Appendix A.3. The result in T_r is

$$\mathcal{L} = \frac{\partial}{\partial\xi}\left((1+\xi)\left[(1-\xi)\frac{\partial}{\partial\xi} - (1+\eta)\frac{\partial}{\partial\eta}\right]\right) + \frac{\partial}{\partial\eta}\left((1+\eta)\left[(1-\eta)\frac{\partial}{\partial\eta} - (1+\xi)\frac{\partial}{\partial\xi}\right]\right). \tag{6}$$

The eigenfunctions of (5) can then be shown to be a tensor product of Jacobi polynomials [6–8]. They are in fact the classical orthogonal polynomials in the triangle, previously obtained without the use of a Sturm–Liouville problem in [9–12]. These polynomials are usually referred to as Dubiner or Proriol polynomials.

The eigenfunctions of Eq. 5 (Dubiner polynomials) are given by

$$g_{mn}(\xi,\eta) = P_m^{0,0}\left(\frac{\xi}{1-\eta}\right)(1-\eta)^m P_n^{2m+1,0}(\eta)$$

for non-negative integers (m,n), where $P_n^{\alpha,\beta}$ are the Jacobi Polynomials with weight (α,β) and degree n. Stable recurrence relations for evaluating these polynomials are given in [13].

In this work, instead of the traditional double index (m,n), we will use a single index given by $i = (m+n+1)(m+n+2)/2 - m$. Using this index, the Dubiner polynomials g_i satisfy

$$\mathcal{L}(g_i) = d_i g_i. \tag{7}$$

The eigenvalues are given by

$$d_i = d_{mn} = -(m+n)(m+n+2).$$

These were first derived in [6], where it was noted that the vector space made up of all eigenfunctions with eigenvalues less than a constant C is the classic polynomial truncation

$$\mathcal{P}_d = \text{span}\{x^n y^m, m+n \le d\}, \tag{8}$$

with $d = \lfloor -1 + \sqrt{1+C} \rfloor$.

2.4 A generalized eigenfunction equation in T_e

The similarities of the Sturm–Liouville equation for the interval (Eq. 1) and the Sturm–Liouville equation in T_e (Eq. 5) suggests a natural form for a Sturm–Liouville equation in T_e. By analogy with the one-dimensional case, it is hoped that the eigenfunctions of this equation would result in a more uniform resolution over the triangle.

We thus want to add a term similar to the $\alpha^2 x^2 u$ term from (1). To ensure our new equation remains invariant under D_3, we write it in the **a**, **b** and **c** coordinate systems,

$$\mathcal{L}(u) - \alpha^2 \frac{1}{3}(a_\perp^2 + b_\perp^2 + c_\perp^2)u = \lambda u. \tag{9}$$

We have added a 1/3 to keep the scaling of α similar to that in (1).

To solve this equation, we again map to T_r and write it as

$$\mathcal{L}(u) - \alpha^2 h u = \lambda u, \tag{10}$$

where $\mathcal{L}$ is given by (6) and

$$h = \frac{1}{2}(x^2+y^2) = \frac{3}{16}\left(\left(\xi + \frac{1}{3}\right)^2 + \left(\eta + \frac{1}{3}\right)^2 + \left(\xi + \eta + \frac{2}{3}\right)^2\right).$$

3 Solving for the eigenfunctions

To solve (10), we use a straightforward generalization of the procedure used in [3] to solve for prolate spheroidal basis functions. We use a Dubiner spectral method, meaning that we replace u in the Sturm–Liouville equation by its expansion in Dubiner polynomials, and then solve for the expansion coefficients.

3.1 Expansion in terms of Dubiner polynomials

We denote the expansion of the unknown eigenfunction u in terms of Dubiner polynomials by

$$u(\xi,\eta) = \sum_{i=1}^{\infty} \tilde{u}(i) g_i(\xi,\eta), \tag{11}$$

where $\tilde{u}(i)$ are the Dubiner coefficients of u. Using (7) and (11), we can rewrite (10) in terms of the Dubiner coefficients and obtain

$$\sum_{i=1}^{\infty} d_i g_i \tilde{u}(i) - \alpha^2 \sum_{i=1}^{\infty} h g_i \tilde{u}(i) = \sum_{i=1}^{\infty} \lambda \tilde{u}(i) g_i.$$

To simplify further, let a_j^i be the Dubiner coefficients of hg_i,

$$a_j^i = \iint_{T_r} hg_i g_j \, \mathrm{d}\xi \, \mathrm{d}\eta \qquad h(\xi,\eta)g_i(\xi,\eta) = \sum_{j=1}^{\infty} a_j^i g_j(\xi,\eta) \tag{12}$$

Substitute this expansion to obtain

$$\sum_{i=1}^{\infty} d_i g_i \tilde{u}(i) - \alpha^2 \sum_{i=1}^{\infty}\sum_{j=1}^{\infty} a_j^i g_j \tilde{u}(i) = \sum_{i=1}^{\infty} \lambda \tilde{u}(i) g_i.$$

Relabeling and then equating coefficients of g_i yields

$$d_i \tilde{u}(i) - \alpha^2 \sum_{j=1}^{\infty} a_i^j \tilde{u}(j) = \lambda \tilde{u}(i). \tag{13}$$

3.2 Numerical approximation

To solve (13) numerically, we work in the truncated polynomial space $\mathcal{P}_d$ given by (8). The dimension of this space is $N = (d+1)(d+2)/2$, and functions in this space are exactly represented by their N Dubiner coefficients. Denote the vector of Dubiner coefficients by

$$\tilde{\mathbf{u}} = \begin{pmatrix} \tilde{u}(1) \\ \tilde{u}(2) \\ \vdots \\ \tilde{u}(N) \end{pmatrix},$$

let D be the $N \times N$ diagonal matrix with entries $D_{ii} = d_i$, and let A be the $N \times N$ matrix with entries $A_{ij} = a_i^j$. Equation (13), written for $\tilde{\mathbf{u}}$ is then

$$\left(D - \alpha^2 A\right) \tilde{\mathbf{u}} = \lambda \tilde{\mathbf{u}}. \tag{14}$$

Since our differential operator $\mathcal{L} - \alpha^2 h$ is by construction self-adjoint, we expect our discretization to preserves this property and thus we take care to ensure that $D - \alpha^2 A$ is symmetric. Then the eigenvectors $\tilde{\mathbf{u}}$ of (14) are real, orthogonal and complete in R^N. By Plancharel's equation, the eigenfunctions obtained by summing the truncated Dubiner series are also exactly orthogonal in the continuous L_2 norm over the triangle.

3.3 Derivation of A

We now describe the procedure used to compute a_i^j, the i'th Dubiner coefficients of hg_j. We are solving (14) in the space $\mathcal{P}_d$, so the polynomials $g_j \in \mathcal{P}_d$ and $hg_j \in \mathcal{P}_{d+2}$. By virtue of (12), we can ensure that A is symmetric if we compute these terms exactly, and thus it is necessary to work in the space $\mathcal{P}_{d+2}$. Let $N' = (d+3)(d+4)/2$ be the dimension of this space, and let $\{(\xi_k, \eta_k)\}$ be a set of N' points in T_r. We can evaluate the polynomial hg_j at the N' points from its Dubiner coefficients by

$$h(\xi_k,\eta_k)g_j(\xi_k,\eta_k) = \sum_{i=1}^{N'} a_i^j g_i(\xi_k,\eta_k). \tag{15}$$

Note that $g_j(\xi_k, \eta_k)$ represents the $N' \times N'$ Vandermonde matrix G of the Dubiner polynomials evaluated at the N' points. If these points are non-degenerate, G will be invertible, and then

$$a_i^j = \sum_k^{N'} G_{ik}^{-1} h(\xi_k, \eta_k) g_j(\xi_k, \eta_k). \tag{16}$$

To compute A, we choose a set of N' non-degenerate points in T_r, form G, then compute G^{-1} applied to hg_j via Gaussian elimination. The N' points must be well conditioned to invert G, so for this we use the Fekete points computed in [14]. The condition number of G for those points is less than 110 for polynomial truncations up to $\mathcal{P}_{30}$ with $N' \leq 496$.

Finally, we note that, because of the recurrence relations used to construct Dubiner polynomials, it can be shown that a quadratic polynomial times a Dubiner polynomial can be expanded in at most 15 other Dubiner polynomials. Thus each column of A will have at most 15 entries.

3.4 Generalized eigenfunctions in T_e

We solve Eq. 14 using Matlab's `eig` routine. Denote the eigenfunctions computed for a given α by $E_k(\xi, \eta; \alpha)$ with eigenvalue λ_k. We define a family of eigenspaces by

$$\Lambda_\alpha(\lambda) = \text{span}\{E_k, \quad \forall \lambda_k = \lambda\}.$$

and define a generalized basis for the triangle by taking the span of all eigenfunctions with eigenvalue less than a constant,

$$\mathcal{E}_\alpha(\lambda) = \bigcup_{\lambda_k \leq \lambda} \Lambda_\alpha(\lambda).$$

In the case $\alpha = 0$, the eigenfunctions are just the first M Dubiner polynomials. The first 15 polynomials are plotted in Fig. 3. For $\lambda = d(d+2)$, the eigenfunctions are the Dubiner polynomials of top degree d, the eigenspace $\Lambda_0(d(d+2))$ is given by the span of all polynomials of top degree d, and $\mathcal{E}_0(d(d+2)) = \mathcal{P}_d$. We note that since the Sturm–Liouville equation (for all α) was constructed to be invariant under D_3, the eigenspaces $\Lambda_\alpha(\lambda)$ must also be invariant under D_3. By this we mean that the rotation or reflection of any function in $\Lambda_\alpha(\lambda)$ by any of the elements of D_3 remains in $\Lambda_\alpha(\lambda)$.

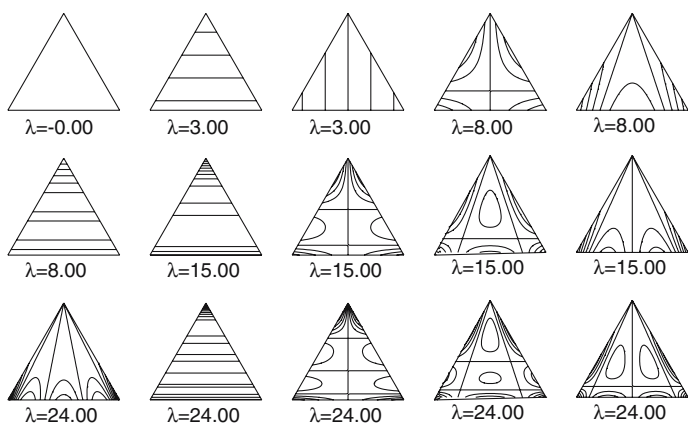

Fig. 3 Contour plots of the first 15 orthonormal eigenfunctions in the triangle for $\alpha = 0$ (for which the eigenfunctions are the Dubiner polynomials up to degree 4). The contour interval is 1.0. Many of the eigenfunctions have strong peaks near the corners

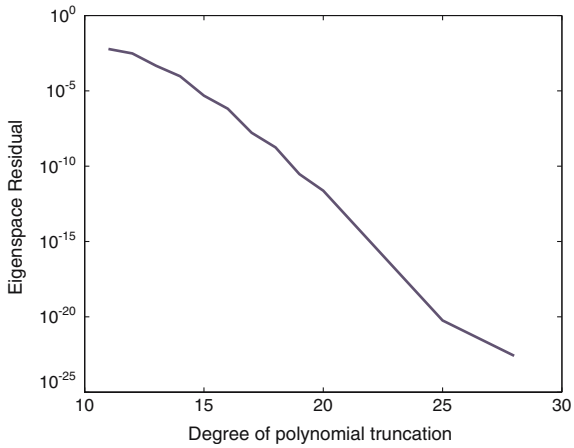

Fig. 4 Exponential convergence of the eigenspace residual, plotted against the polynomial truncation used to represent the eigenfunctions. The eigenspace is the first 66 eigenfunctions for $\alpha = 10$. The residual for this space is defined in Eq. 17

We estimate the convergence properties of our algorithm by using the solutions from (14) and computing their residual using (10). Since our numerically computed eigenfunctions are given by a polynomial of finite degree, the terms in (10) can be computed exactly and thus the residual is also computed exactly. For an eigenspace $\mathcal{E}_\alpha$, we define the residual by

$$\max_{E_k \in \mathcal{E}_\alpha} \frac{\iint_{T_r} \left(\frac{1}{\lambda_k} \left(\mathcal{L}(E_k) - \alpha^2 h E_k \right) - E_k \right)^2}{\iint_{T_r} E_k^2}. \tag{17}$$

To demonstrate the convergence of our algorithm, we take $\alpha = 10$ and $M = 66$. This would represent polynomials up to degree 10 for the case of $\alpha = 0$. In Fig. 4, we plot the residual for $\mathcal{E}_\alpha$ as a function of degree d of the polynomial space $\mathcal{P}_d$ used to compute the eigenfunctions E_k^α. Note that the plot is log-linear, illustrating the spectral convergence in the truncation dimension d. Since the matrix is symmetric, the Rayleigh quotient argument shows that eigenvalues will converge at an even faster rate.

In this work, all eigenfunctions were computed such that their residual is less than 1×10^{-12}.

The first 15 eigenfunctions for $\alpha = 5, 10$ and 15 are plotted in Figs. 5, 6, and 7. They are all normalized so that

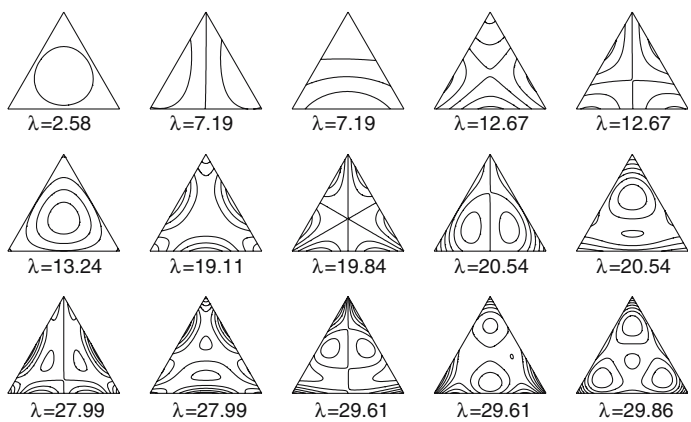

Fig. 5 Contour plots of the first 15 orthonormal eigenfunctions in the triangle for $\alpha = 5$. The contour interval is 1.0. Note that the eigenspaces for a given eigenvalue are now all of dimension one or two. This appears to occur for all $\alpha > 0$

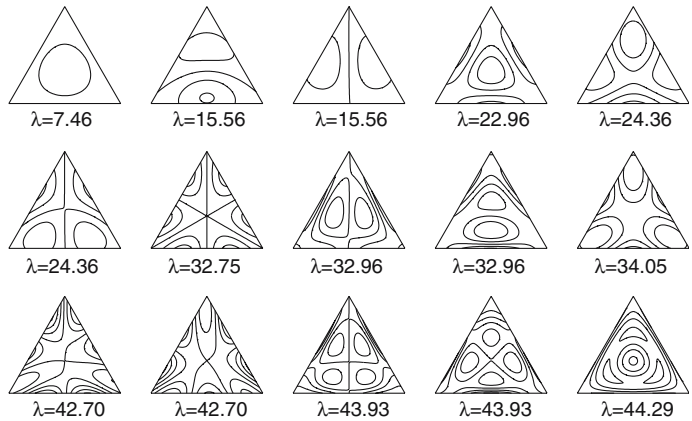

Fig. 6 Contour plots of the first 15 orthonormal eigenfunctions in the triangle for $\alpha = 10$. The contour interval is 1.0

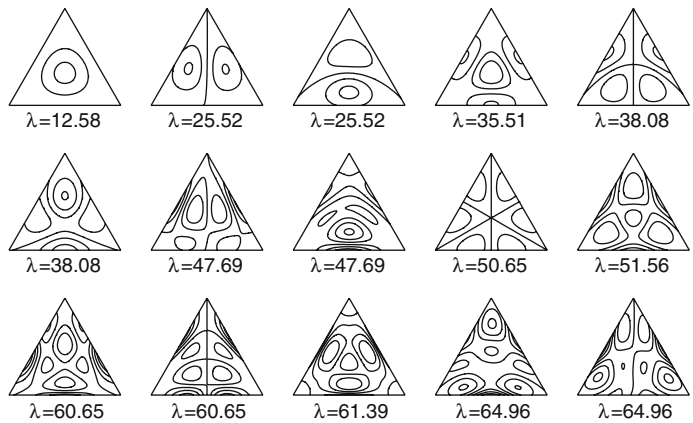

Fig. 7 Contour plots of the first 15 orthonormal eigenfunctions in the triangle for $\alpha = 15$. The contour interval is 1.0. Note that the clustering of contours near the boundaries is much reduced over the case $\alpha = 0$ (Dubiner polynomials) case

$$\iint_{T_r} E_k^2 = 1.$$

Visually, the graphs appear to confirm that increasing α leads to eigenfunctions with more uniform resolution. For $\alpha = 10$ and 15, the length scale of the oscillations is clearly larger than that for $\alpha = 0$. Also, the contours are not as closely spaced near the boundary of the triangle, showing that the gradients are less steep and the magnitude is reduced. For $\alpha = 0$, the normalized eigenfunctions have values that exceed 10 in the corners of the triangle, while for $\alpha = 15$, the maximum value is less than four.

One interesting difference between $\alpha = 0$ and $\alpha > 0$ concerns the dimension of the eigenspaces $\Lambda_\alpha(\lambda_k)$. As previously mentioned, for $\alpha = 0$, the eigenvalues are integers, and the kth eigenspace is the span of all polynomials of top degree $k - 1$. The kth eigenspace, as α is increased from 0, breaks into a collection of eigenspaces of dimension 2, except when k is odd, in which case there will also be one eigenspace of dimension one.

Finally, we note that just as with the PSWFs, the constant function is not in any finite truncation of the $\alpha > 0$ eigenfunctions.

4 Approximation results

To demonstrate that the resolution of the eigenfunctions is more uniform for $\alpha > 0$, we consider the accuracy of truncated eigenfunction expansions of sinusoids. Consider the uniformly oscillating function in T_e,

$$f(x,y) = \sin\left(\frac{\pi}{2}kx\right)\sin\left(\frac{\pi}{2}ky\right) = \sin\left(\frac{\pi}{2}k\left(\frac{\sqrt{3}}{2}\xi + \frac{\sqrt{3}}{4}\eta + \frac{\sqrt{3}}{4}\right)\right)\sin\left(\frac{\pi}{2}k\left(\frac{3}{4}\eta + \frac{1}{4}\right)\right).$$

Its expansion in terms of the first M eigenfunctions of (14) is given by

$$\tilde{f}(\xi,\eta) = \sum_{k=1}^{M}\hat{f}(k)E_k(\xi,\eta;\alpha), \quad \hat{f}(k) = \iint_{T_r} f(\xi,\eta)E_k(\xi,\eta;\alpha).$$

We compute the expansion coefficients $\hat{f}(k)$ numerically to a precision of 10^{-10}. For convenience, we only use truncated expansions where $M = d(d+1)$ for integer d. Thus for $\alpha = 0$ the expansion in M polynomials is the traditional degree d polynomial expansion of f. For $\alpha > 0$, these are no longer polynomial expansions; however, we still consider them expansions of quasi-degree d.

We compute the L_2 norm of the difference between f and its truncated expansion. Denote this residual by R,

$$R(k,M,\alpha) = \iint_{T_r}(f-\tilde{f})^2,$$

regarded as a function of the wave number, k, the number of terms in the expansion, M, and the value of the bandwidth parameter, α. To examine this error, we first consider the case with $k = 3$ and contour R as a function of M and α, shown in Fig. 8. As expected, for any fixed α, as the number of terms M in the expansion is increased, the error decays rapidly, indicating the spectral convergence of these eigenfunctions. More interesting, consider a fixed M as α is increased. Here we see that for this choice of f, there is

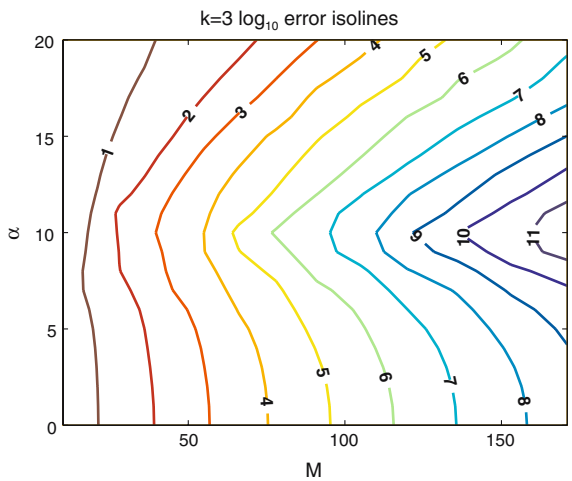

Fig. 8 Error in the M-term eigenfunction expansion of $\sin\pi 3x/2\sin\pi 3y/2$, contoured as a function of M and parameter α. Note that, for a fixed M, the optimal α will reduce the error nearly by two orders of magnitude

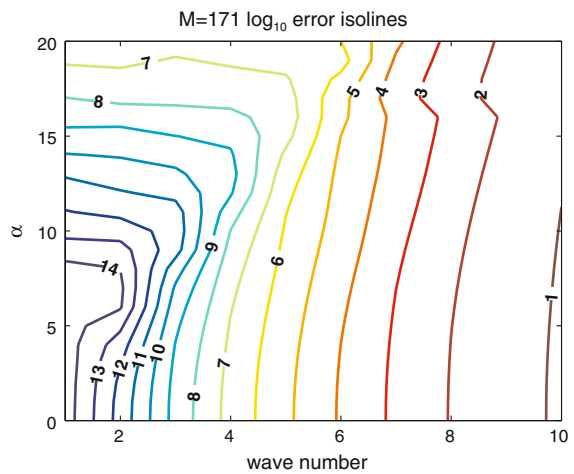

Fig. 9 The error in the 171-term (quasi-degree 17) eigenfunction expansion of $\sin\pi kx/2\sin\pi ky/2$, contoured as a function of wave number k and parameter α. Note that, for any k, there is an optimal α which grows with k

an optimal value of $\alpha = 10$ where the error is reduced significantly as compared to that for $\alpha = 0$. For the larger values of M, the error in the expansion is reduced by three orders of magnitude as α is increased from 0 to 10.

In Fig. 9 we contour the same residual R, but this time with $M = 171$ and R treated as a function of wave number k and bandwidth parameter α. This plot should be compared to that shown in Fig. 5 of [2]. The results are quite similar. In particular, for each k, there is optimal bandwidth parameter $\alpha > 0$ that has a significantly lower error when compared to $\alpha = 0$. But as α is further increased, the error increases until it becomes O(1). The plot also shows that the optimal value of α increases with k. This suggests that the Anti-theorem 7.1 of [2] also applies to these eigenfunctions in the triangle: *In approximating* $\exp(ikx)$*, reduced error for moderate wave numbers k may be purchased at the price of increased error for small wave numbers.*

Thus, we have evidence to support a conclusion similar to that obtained in [2, 5] for approximating functions f: In the over-resolved case, where the Fourier transform of f falls sufficiently fast, then the $\alpha > 0$ eigenfunction expansion of f will not be as accurate as the $\alpha = 0$ case. However, if the Fourier transform of f decays at a slow rate, then to achieve a given level of accuracy requires the accurate resolution of moderate wave numbers k. In this regime, the $\alpha > 0$ eigenfunctions give significant improvements over the $\alpha = 0$ eigenfunctions.

We now consider the approximation error for a function which is singular outside the triangle. Modeled after the example in [2], we look at a function of the form

$$f(x, y) = \frac{1}{x^2 + y^2 + \gamma^2}$$

for pole location parameter γ. The complex valued singularities of this function are at $y = \pm i\sqrt{x^2 + \gamma^2}$. The error is shown in Fig. 10, where we contour the residual R, as a function of pole location parameter γ and bandwidth parameter α, with $M = 171$. This plot should be compared to that shown for the one-dimensional results in Fig. 10 of [2]. The results are similar: adjusting α results in only a small reduction in the error for small values of γ. For larger values of γ, there is an optimal value of α, but the gain is small compared to the improvement seen when approximating sinusoids. Furthermore, for α larger than the optimal value, the error decreases quickly, so as pointed out in [2], there is only a small margin of error in choosing α.

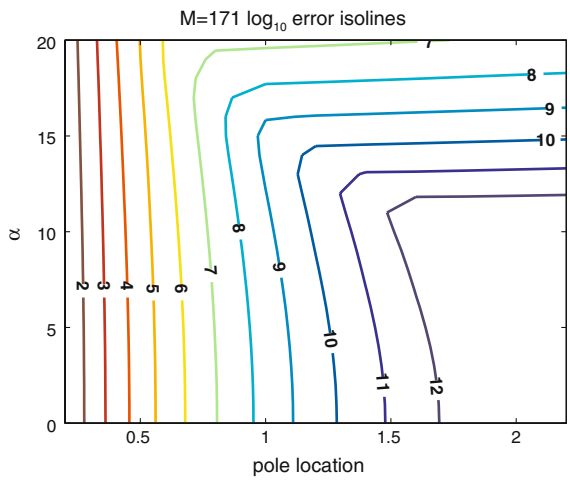

Fig. 10 The error in the 171-term (quasi-degree 17) eigenfunction expansion of $1/(x^2 + y^2 + \gamma^2)$, contoured as a function of pole location γ and parameter α. Note that for any γ there is an optimal α which minimized the error, but if α is chosen slightly larger than the optimal value, the error increases dramatically

5 Conclusion

Based on the one-dimensional Sturm–Liouville equation for the PSWFs, we have generalized the Sturm–Liouville equation for the Dubiner polynomials in the triangle. The result is a one-parameter family of eigenfunctions. As the bandwidth parameter α is increased, the eigenfunctions appear to have a more uniform resolution in the triangle, as shown by the fact that they better approximate the uniform oscillations of sinusoids. Key properties of the original ($\alpha = 0$) Sturm–Liouville eigenfunctions are retained: the functions are orthogonal, invariant under D_3, and so the truncated eigenfunction expansions converge faster than any polynomial for smooth functions in the triangle independent of their boundary conditions.

As in the case of PSWFs [5], it is expected that these functions can lead to improvements for numerical methods that rely on triangular domains or elements. Because these functions are expressed in terms of the commonly used Dubiner polynomials, any existing code which uses Dubiner polynomials can be easily modified to instead use a basis made up of linear combinations of Dubiner polynomials. However, for nodal based algorithms, one difficulty remains: suitable collocation points with optimal interpolation and quadrature properties for these new eigenspaces will need to be computed. Because of the evidence presented here, we conjecture that these collocation points would have less clustering at the boundaries of the triangle when compared to optimal polynomial interpolation points.

Appendix: Algebraic formulas for $\mathcal{L}$ in T_e and T_r

A.1 The operator $\mathcal{L}_a$ is self-adjoint and negative-definite

Proof: We start with the following integral, for a fixed a, and integrate by parts. Let $u, v \in H^2(T_e)$.

$$
\begin{aligned}
&\int_{-(a-1)/\sqrt{3}}^{(a-1)/\sqrt{3}} \mathcal{L}_a(u) v \, \mathrm{d}a_\perp \\
&\quad = \int_{-(a-1)/\sqrt{3}}^{(a-1)/\sqrt{3}} \frac{\partial}{\partial a_\perp} \left(p(a, a_\perp) \frac{\partial u}{\partial a_\perp} \right) v \, \mathrm{d}a_\perp \\
&\quad = \int_{-(a-1)/\sqrt{3}}^{(a-1)/\sqrt{3}} -p(a, a_\perp) \frac{\partial u}{\partial a_\perp} \frac{\partial v}{\partial a_\perp} \, \mathrm{d}a_\perp + \left[p(a, a_\perp) \frac{\partial u}{\partial a_\perp} v \right]_{a_\perp = -(a-1)/\sqrt{3}}^{a_\perp = (a-1)/\sqrt{3}} \\
&\quad = \int_{-(a-1)/\sqrt{3}}^{(a-1)/\sqrt{3}} u \frac{\partial}{\partial a_\perp} \left(p(a, a_\perp) \frac{\partial v}{\partial a_\perp} \right) \mathrm{d}a_\perp + \left[p(a, a_\perp) \frac{\partial v}{\partial a_\perp} u + p(a, a_\perp) \frac{\partial u}{\partial a_\perp} v \right]_{a_\perp = -(a-1)/\sqrt{3}}^{a_\perp = (a-1)/\sqrt{3}} \\
&\quad = \int_{-(a-1)/\sqrt{3}}^{(a-1)/\sqrt{3}} \mathcal{L}_a(v) u \, \mathrm{d}a_\perp .
\end{aligned}
$$

The boundary terms vanishes since $p(a, a_\perp)$ is zero at both end-points. The integral over T_e is given by

$$
\iint_{T_e} = \int_{-1/2}^{1} \int_{-(a-1)/\sqrt{3}}^{(a-1)/\sqrt{3}} \mathrm{d}a_\perp \, \mathrm{d}a,
$$

so we have that

$$
\iint_{T_e} \mathcal{L}_a(u) v = \iint_{T_e} \mathcal{L}_a(v) u.
$$

If we assume that $p > 0$ in T_e, then integration by parts only once shows that $\mathcal{L}_a$ is negative definite,

$$
\int_{-(a-1)/\sqrt{3}}^{(a-1)/\sqrt{3}} \mathcal{L}_a(u) u \, \mathrm{d}a_\perp = - \int_{-(a-1)/\sqrt{3}}^{(a-1)/\sqrt{3}} p(a, a_\perp) \left(\frac{\partial u}{\partial a_\perp} \right)^2 \mathrm{d}a_\perp \le 0,
$$

and thus

$$\iint_{T_e} \mathcal{L}_a(u)u \leq 0,$$

where equality is only obtained if $\frac{\partial u}{\partial a_\perp}$ is zero almost everywhere.

A.2 Mapping T_e to T_r

To map T_e (given in Fig. 1) to T_r (given in Fig. 2), we use

$$\xi = \tfrac{2\sqrt{3}}{3}x - \tfrac{2}{3}y - \tfrac{1}{3}, \quad x = \frac{\sqrt{3}}{2}\xi + \frac{\sqrt{3}}{4}\eta + \frac{\sqrt{3}}{4}, \tag{18}$$

$$\eta = \tfrac{4}{3}y - \tfrac{1}{3}, \qquad y = \frac{3}{4}\eta + \frac{1}{4}. \tag{19}$$

The various coordinate systems in T_e are related by

$$a = y, \quad b = -\frac{\sqrt{3}}{2}x - \frac{1}{2}y, \quad c = \frac{\sqrt{3}}{2}x - \frac{1}{2}y, \tag{20}$$

$$a_\perp = x, \quad b_\perp = -\frac{1}{2}x + \frac{\sqrt{3}}{2}y, \quad c_\perp = -\frac{1}{2}x - \frac{\sqrt{3}}{2}y, \tag{21}$$

and in T_r by,

$$a = \frac{3}{4}\eta + \frac{1}{4}, \quad b = -\frac{3}{4}\xi - \frac{3}{4}\eta - \frac{1}{2}, \quad c = \frac{3}{4}\xi + \frac{1}{4}, \tag{22}$$

$$a_\perp = \frac{\sqrt{3}}{2}\xi + \frac{\sqrt{3}}{4}\eta + \frac{\sqrt{3}}{4}, \quad b_\perp = -\frac{\sqrt{3}}{4}\xi + \frac{\sqrt{3}}{4}\eta, \quad c_\perp = -\frac{\sqrt{3}}{4}\xi - \frac{\sqrt{3}}{2}\eta - \frac{\sqrt{3}}{4}. \tag{23}$$

A useful identity is

$$a^2 + b^2 + c^2 = a_\perp^2 + b_\perp^2 + c_\perp^2 = \frac{3}{2}x^2 + \frac{3}{2}y^2 = \frac{9}{16}\left(\left(\frac{1}{3} + \xi\right)^2 + \left(\frac{1}{3} + \eta\right)^2 + \left(\frac{2}{3} + \xi + \eta\right)^2\right). \tag{24}$$

We also derive:

$$p(a, a_\perp) = \frac{9}{4}(-\xi - \eta)(\xi + 1), \tag{25}$$

$$p(b, b_\perp) = \frac{9}{4}(\xi + 1)(\eta + 1), \tag{26}$$

$$p(c, c_\perp) = \frac{9}{4}(-\xi - \eta)(\eta + 1). \tag{27}$$

The terms in parenthesis are all positive for $(\xi, \eta) \in T_r$, and thus $p > 0$ in T_e.

Now we turn to the differential operators. By the chain rule,

$$\frac{\partial}{\partial x} = \frac{2\sqrt{3}}{3}\frac{\partial}{\partial \xi}, \qquad \frac{\partial}{\partial y} = -\frac{2}{3}\frac{\partial}{\partial \xi} + \frac{4}{3}\frac{\partial}{\partial \eta}.$$

Using (2), we have

$$\frac{\partial}{\partial a_\perp} = \frac{\partial}{\partial x} = \frac{2\sqrt{3}}{3}\frac{\partial}{\partial \xi}, \tag{28}$$

$$\frac{\partial}{\partial b_\perp} = -\frac{1}{2}\frac{\partial}{\partial x} + \frac{\sqrt{3}}{2}\frac{\partial}{\partial y} = -\frac{2\sqrt{3}}{3}\frac{\partial}{\partial \xi} + \frac{2\sqrt{3}}{3}\frac{\partial}{\partial \eta}, \tag{29}$$

$$\frac{\partial}{\partial c_\perp} = -\frac{1}{2}\frac{\partial}{\partial x} - \frac{\sqrt{3}}{2}\frac{\partial}{\partial y} = -\frac{2\sqrt{3}}{3}\frac{\partial}{\partial \eta}. \tag{30}$$

The second derivatives are then given by

$$\frac{\partial^2}{\partial a_\perp^2} = \frac{4}{3}\frac{\partial^2}{\partial \xi^2}, \tag{31}$$

$$\frac{\partial^2}{\partial b_\perp^2} = \frac{4}{3}\frac{\partial^2}{\partial \xi^2} - \frac{8}{3}\frac{\partial}{\partial \xi}\frac{\partial}{\partial \eta} + \frac{4}{3}\frac{\partial^2}{\partial \eta^2}, \tag{32}$$

$$\frac{\partial^2}{\partial c_\perp^2} = \frac{4}{3}\frac{\partial^2}{\partial \eta^2}. \tag{33}$$

A.3 Transformation of $\mathcal{L}$ from T_e to T_r

We show how the operator $\mathcal{L}$ is transformed by the mapping of T_e to T_r. Starting with

$$\mathcal{L} = \frac{1}{3}p(a,a_\perp)\frac{\partial^2}{\partial a_\perp^2} - 2a_\perp\frac{\partial}{\partial a_\perp} + \frac{1}{3}p(b,b_\perp)\frac{\partial^2}{\partial b_\perp^2} - 2b_\perp\frac{\partial}{\partial b_\perp} + \frac{1}{3}p(c,c_\perp)\frac{\partial^2}{\partial c_\perp^2} - 2c_\perp\frac{\partial}{\partial c_\perp},$$

we first derive

$$\begin{aligned} -2\left(a_\perp\frac{\partial}{\partial a_\perp} + b_\perp\frac{\partial}{\partial b_\perp} + c_\perp\frac{\partial}{\partial c_\perp}\right) &= -\frac{4\sqrt{3}}{3}\left((a_\perp - b_\perp)\frac{\partial}{\partial \xi} + (b_\perp - c_\perp)\frac{\partial}{\partial \eta}\right) \\ &= -(3\xi+1)\frac{\partial}{\partial \xi} - (3\eta+1)\frac{\partial}{\partial \eta}, \end{aligned} \tag{34}$$

and then derive

$$\begin{aligned} &\frac{1}{3}\left(p(a,a_\perp)\frac{\partial^2}{\partial a_\perp^2} + p(b,b_\perp)\frac{\partial^2}{\partial b_\perp^2} + p(c,c_\perp)\frac{\partial^2}{\partial c_\perp^2}\right) \\ &\quad = \frac{4}{9}\left((p(a,a_\perp) + p(b,b_\perp))\frac{\partial^2}{\partial \xi^2} + (p(b,b_\perp) + p(c,c_\perp))\frac{\partial^2}{\partial \eta^2} - 2p(b,b_\perp)\frac{\partial}{\partial \xi}\frac{\partial}{\partial \eta}\right) \\ &\quad = (1-\xi^2)\frac{\partial^2}{\partial \xi^2} + (1-\eta^2)\frac{\partial^2}{\partial \eta^2} - 2(1+\xi)(1+\eta)\frac{\partial}{\partial \xi}\frac{\partial}{\partial \eta}. \end{aligned} \tag{35}$$

Combining these results, we find

$$\begin{aligned} \mathcal{L} &= (1-\xi^2)\frac{\partial^2}{\partial \xi^2} + (1-\eta^2)\frac{\partial^2}{\partial \eta^2} - 2(1+\xi)(1+\eta)\frac{\partial}{\partial \xi}\frac{\partial}{\partial \eta} - (3\xi+1)\frac{\partial}{\partial \xi} - (3\eta+1)\frac{\partial}{\partial \eta} \\ &= \frac{\partial}{\partial \xi}\left(\left[(1-\xi^2)\frac{\partial}{\partial \xi} - (1+\xi)(1+\eta)\frac{\partial}{\partial \eta}\right]\right) + \frac{\partial}{\partial \eta}\left(\left[(1-\eta^2)\frac{\partial}{\partial \eta} - (1+\xi)(1+\eta)\frac{\partial}{\partial \xi}\right]\right) \\ &= \frac{\partial}{\partial \xi}\left((1+\xi)\left[(1-\xi)\frac{\partial}{\partial \xi} - (1+\eta)\frac{\partial}{\partial \eta}\right]\right) + \frac{\partial}{\partial \eta}\left((1+\eta)\left[(1-\eta)\frac{\partial}{\partial \eta} - (1+\xi)\frac{\partial}{\partial \xi}\right]\right). \end{aligned}$$

For completeness, we also give $\mathcal{L}$ written in Cartesian coordinates in T_e:

$$\mathcal{L} = \frac{\partial}{\partial x}\left(\left(x^2 - \frac{1}{2}y + \frac{1}{2}\right)\frac{\partial}{\partial x} - x\left(y + \frac{1}{2}\right)\frac{\partial}{\partial y}\right) + \frac{\partial}{\partial y}\left(\left(-y^2 + \frac{1}{2}y + \frac{1}{2}\right)\frac{\partial}{\partial y} - x\left(y + \frac{1}{2}\right)\frac{\partial}{\partial x}\right). \tag{36}$$

References

1. Xiao H, Rokhlin V, Yarvin N (2001) Prolate spheroidal wavefunctions, quadrature and interpolation. Inverse Problems 17:805–838
2. Boyd JP (2004) Prolate spheroidal wavefunctions as an alternative to chebyshev and legendre polynomials for spectral and pseudospectral algorithms. J Comp Phys 199:688–716
3. Boyd JP (2004) Computation of grid points, quadrature weights and derivatives for spectral element methods using prolate spheroidal wave functions — prolate elements. ACM Trans Comp Logic 31:149–165
4. Beylkin G, Sandberg K (2005) Wave propagation using bases for bandlimited functions. Wave Motion 41:263–291
5. Chen QY, Gottlieb D, Hesthaven JS (2005) Spectral methods based on prolate spheroidal wave functions for hyperbolic pdes. SIAM J Num Anal 43:1912–1933
6. Wingate BA, Taylor MA (1998) The natural function space for triangular and tetrahedral spectral elements. Technical Report LA-UR-98-1711, Los Alamos National Laboratory
7. Owens RG (1998) Spectral approximations on the triangle. Proc Roy Soc Lond A, 454:857–872
8. Braess D, Schwab C (2000) Approximation on simplices with respect to weighted Sobolev norms. J Approx Theory 103(2):329–337
9. Proriol J (1957) Sur une famille de polynomes à deux variables orthogonaux dans un triangle. Comptes Rendus de l'Académie des Sciences Paris 245:2459–2461
10. Appell P, Feriet JK (1926) Function hypergeometriques et hyperspheriques polynomials d'Hermite. Gauthier-villars, Paris, FR
11. Koornwinder T (1975) Two-variable analogues of the classical orthogonal polynomials. In: Askey RA (ed) Theory and applications of special functions. Academic Press, pp. 435–495
12. Dubiner M (1991) Spectral methods on triangles and other domains. J Sci Comp 6:345–390
13. Sherwin SJ, Karniadakis GE (1995) A triangular spectral element method; applications to the incompressible Navier-Stokes equations. Comp Meth Appl Mech Eng 123:189–229
14. Taylor MA, Wingate BA, Vincent R (2000) An algorithm for computing Fekete points in the triangle. SIAM J Numer Anal 38:1707–1720